J. Micropalaeontology, 45, 297–308, 2026
https://doi.org/10.5194/jm-45-297-2026

Journal of Micropalaeontology
Open Access

Planktic foraminiferal distribution across the Cretaceous–Paleogene (K–Pg) boundary from the Neuquén Basin (Cerro Azul section): biostratigraphy and paleoenvironmental significance

Guilherme Krahl[1], Andrea Concheyro[2,3], Marlone H. H. Bom[1], Rodrigo M. Guerra[1,4], Karlos G. D. Kochhann[1,5], Thorsten Bauersachs[6], Lorenz Schwark[7], Daiane Ceolin[1], Telma Musso[8], and Gerson Fauth[1]

[1]Technological Institute for Paleoceanography and Climate Change (itt OCEANEON), UNISINOS University, São Leopoldo, Brazil
[2]Instituto Antártico Argentino (IAA), Buenos Aires, Argentina
[3]IDEAN-CONICET, Departamento de Ciências Geológicas, Universidade de Buenos Aires, Pavilhão II, Cidade Universitária, 1428, Buenos Aires, Argentina
[4]Museu Itinerante de Ciências Naturais, Rua Buarque de Macedo, 4242, sala 1, Carlos Barbosa, RS, Brazil
[5]GEOMAR Helmholtz Centre for Ocean Research Kiel, Kiel, Germany
[6]RWTH Aachen University, Institute for Organic Biogeochemistry in Geo-Systems, Aachen, Germany
[7]Christian-Albrechts-University, Institute of Geosciences, Ludewig-Meyn-Straße 10, 24118 Kiel, Germany
[8]CONICET, Instituto de Investigação e Desenvolvimento em Engenharia de Processos, Biotecnologia e Energias Alternativas e Faculdade de Engenharia e Universidade Nacional del Comahue, Buenos Aires 1400, 8300 Neuquén, Argentina

Correspondence: Guilherme Krahl (gkrahl@unisinos.br)

Received: 8 August 2025 – Revised: 23 February 2026 – Accepted: 23 March 2026 – Published: 15 April 2026

Abstract. The Maastrichtian–Danian time interval corresponds to one of the largest mass extinctions in the Earth's geological history. We investigate changes in planktic foraminiferal assemblages and TEX_{86}^{H}-based sea surface temperatures (SSTs), which reflect surface water conditions, across the Maastrichtian–Danian transition at the Cerro Azul section in the Neuquén Basin, Argentina. Within the Maastrichtian, we identify species that became extinct at the Cretaceous–Paleogene (K–Pg) boundary, such as *Planoheterohelix globulosa* and *Muricohedbergella monmouthensis*, even though these taxa are not typically employed as biostratigraphic markers. Dominance of guembelitrids, usually characterised as opportunistic taxa, is recognised in the upper Maastrichtian interval and within the first 35 cm of the lower Danian, suggesting broad instability in the water column across the K–Pg boundary. Within the lower Danian, two planktic foraminiferal biozones, with high-latitude paleogeographic affinities, were recognised. The AP0 zone was recognised for the lowermost 45 cm above the K–Pg boundary, within the partial range of *Turborotalina nikolasi*. The first occurrence of *Globoconusa daubjergensis*, 45 cm above the K–Pg boundary, defines the base of subzone AP1a, which extends towards the top of the studied interval (90 cm above the K–Pg boundary). The planktic foraminiferal fauna recovered from the early Danian interval exhibits a strong affinity to high latitudes, as evidenced by the presence of *Antarcticella pauciloculata*. However, at 45 cm above the K–Pg boundary (biozone AP1a), a slight increase in the abundance and/or appearance of tropical and/or subtropical species (*Woodringina claytonensis*) is observed, suggesting an increase in surface water temperature (SST). This coincides with the trend recorded by TEX_{86}^{H}, which shows a $\sim$1.5 °C rise in SST above $\sim$45 cm into the Danian interval at the Cerro Azul section. Our assessment of planktic foraminiferal assemblages suggests that the Cerro Azul section comprises a continuous record of the Maastrichtian and early Danian time interval in the Southern Hemisphere. Additionally, a typical distribution

pattern across the K–Pg boundary is observed, with the bloom of opportunist taxa. The middle- to high-latitude paleobiogeographic affinity observed at the beginning of the Danian period for planktonic foraminiferal assemblages from the Cerro Azul section is based on the occurrence of *Antarcticella paucicloculata*, which has its paleobiogeographic range in the South Atlantic Ocean extended to mid-latitudes.

1 Introduction

The transition from the Maastrichtian to the Danian age was characterised by one of the most intense mass extinction events in Earth's history (Vandenberghe et al., 2012). This extinction represents a planetary-scale disturbance, caused by an asteroid impact on the Yucatan Peninsula and magnified by intensified volcanic activity of the Deccan Traps (e.g. Krahl et al., 2023), which triggered one of the most significant biological crises. In the geological record, it defines the boundary between the Mesozoic and Cenozoic eras, known as the Cretaceous–Paleogene (K–Pg) boundary (Molina, 2015). Planktic foraminifera were particularly affected, with the abrupt loss of over 90 % of Maastrichtian species (e.g. Olsson et al., 1999; Lowery et al., 2020). The few surviving species, however, eventually gave rise to all subsequent Cenozoic lineages (Aze et al., 2011).

The planktic foraminiferal fauna of the earliest Danian wwas characterised by low diversity, high dominance of a few species, rapid evolutionary turnover (Arenillas et al., 2000; Huber et al., 2020; Lowery et al., 2021), and blooms of smaller generalist or opportunist species that thrived under environmental stress (Punekar et al., 2014). Two of the main characteristics of the planktic foraminiferal assemblages after the K–Pg boundary were the occurrence of a Guembelitriid bloom (e.g. Kroon and Nederbragt, 1990; Pardo and Keller, 2008; Punekar et al., 2014) and increased abundance of aberrant species (e.g. Arenillas et al., 2018; Gilabert et al., 2021a, b; Krahl et al., 2023), both indicators of significant environmental stress.

Numerous studies have focused on planktic foraminiferal assemblages across the K–Pg boundary in the South Atlantic Ocean. Paleogeographically, these studies form a transect from low to high latitudes: Poty quarry – northeast of Brazil (Koutsoukos, 1996); Campos Basin (Koutsoukos, 2014); Deep Sea Drilling Project (DSDP) Site 356 – São Paulo Plateau (Krahl et al., 2017); Integrated Ocean Drilling Program (IODP) Site 1262 – Walvis Ridge (Krahl et al., 2023); Ocean Drilling Program (ODP) Site 690 – Maud Rise (Stott and Kennett, 1990; Huber et al., 2020); and Seymour Island, Antarctic Peninsula (Huber, 1988). The occurrences of planktic foraminifera with different latitudinal preferences, likely influenced by sea surface temperature (SST) gradients, affected the presence and/or absence of the taxa used for biostratigraphic subdivision of the Danian strata at high (Huber and Quillévéré, 2005; Huber et al., 2020) and low to middle latitudes (Berggren et al., 1995; Wade et al., 2011).

The Neuquén Basin (Argentina) contains significant exposures of upper Cretaceous and lower Paleogene strata and has been studied for its foraminiferal content (Nañez and Concheyro, 1996; Keller et al., 2007), as well as paleoclimatic and paleoenvironmental dynamics (e.g. Keller et al., 2007; Woelders et al., 2017). Its position at $\sim 45°$ S paleolatitude (van Hinsbergen et al., 2015) is fundamental for understanding the paleobiogeography of planktic foraminifera in the South Atlantic Ocean (e.g. Huber et al., 2020). Keller et al. (2007), studying samples from the Bajada del Jagüel (BJ) section, Neuquén Basin, considered Danian taxa similar to those found at middle and low latitudes and were able to correlate them to global biostratigraphic schemes (e.g. Keller et al., 1996). These authors consider the K–Pg boundary interval to be absent at the BJ section due to a disconformity that extended from the end of the Maastrichtian to the beginning of the Danian (Keller et al., 2007). Nañez and Concheyro (1996) report planktic foraminiferal occurrences for the Opaso, Bajada del Jagüel, and Puesto Sin Nombre sections, which characterised the P1 biozone (Berggren et al., 1995) for the lower Danian strata. It is noteworthy that the occurrence of the P1 biozone had been previously reported by Bertels (1964, 1969a, b, 1970, 1972, 1974, 1975a, b), who identified the *Globigerina pseudobulloides* subzone (equivalent to *Parasubbotina pseudobulloides*) and the upper part of the *Subottina triloculinoides* subzone (Berggren, 1969). Bertels (1964, 1969a, b, 1970, 1972, 1974, 1975a, b) also suggested the presence of a hiatus between Maastrichtian and Danian strata in the Neuquén Basin.

The Cerro Azul section represents one of the most complete records of the K–Pg boundary known in South America (Guerra et al., 2021). However, micropaleontological studies across the K–Pg boundary at the Cerro Azul section are limited to calcareous nannofossils (Guerra et al., 2021), ostracods (Ceolin et al., 2015; Ceolin et al., 2016), and palynomorphs (Pincheira and di Pasquo, 2021). This study presents a detailed analysis of planktic foraminiferal occurrences and a new TEX_{86}^{H}-based SST record across the K–Pg boundary at the Cerro Azul section, allowing for biostratigraphic, paleoenvironmental, and paleobiogeographic interpretations. The results were then compared with previous paleoenvironmental proxy data for this site. The Cerro Azul section provides a valuable opportunity to study the response of planktic foraminifera to the environmental changes at the

K–Pg boundary in mid-latitude regions of the South Atlantic Ocean.

2 Materials and methods

Our study examines a sedimentary succession spanning the K–Pg boundary at the Cerro Azul section in the Neuquén Basin, Argentina (Fig. 1). This section has been the subject of several studies examining sediment geochemistry and the biostratigraphy of calcareous nannofossils (Musso et al., 2012; Guerra et al., 2021). Guerra et al. (2021) reported the record of a complete K–Pg transition (from samples CA1 to CA18) between calcareous nannofossil biozones CC26b and NP1 and geochemistry proxies (e.g. Log(Cr+Co)/Rb). Here, we examined a 1.10 m long interval, with a sampling resolution of 10 cm, between samples CA7 to CA17 of Guerra et al. (2021). Lithologically, the section is composed of yellow-greyish calcareous mudstone in the upper Maastrichtian, overlain by an olive-grey calcareous mudstone at the base of the Paleocene.

2.1 Planktic foraminiferal analysis

Recovery of microfossils involved the following steps: (i) weighing ∼ 10 g of bulk sample, (ii) mechanical breakdown of the sample, (iii) immersion of the sediments in hydrogen peroxide (H_2O_2 at 29 %) for 24 h, (iv) washing residues over a 38 µm mesh sieve, and (v) picking of ∼ 300 planktic foraminiferal specimens under a microscope Zeiss Discovery V.8. For taxonomic identifications, we used the classification schemes of Olsson et al. (1999), Liu and Olsson (1992), Koutsoukos (2014), and Huber et al. (2020). Biostratigraphic interpretations were based on the zonal scheme of Huber and Quillévéré (2005), revised by Huber et al. (2020). All planktic foraminiferal species illustrated in scanning electron micrographs (SEMs), recovered from the Cerro Azul section, are housed in the Paleontological Collections Repository of the Universidad de Buenos Aires, Argentina, under the collection numbers LM-FCEM–4000 to LM-FCEM–4011.

2.2 Glycerol dialkyl glycerol tetraether (GDGT) analysis

Detection of isoGDGTs and brGDGTs (with GDGT denoting glycerol dialkyl glycerol tetraether) was achieved using a Waters Alliance 2695 high-performance liquid chromatograph (HPLC) coupled to a Micromass ZQ single-quadrupole mass spectrometer (MS). The HPLC was fitted with two Waters BEH HILIC columns (2.1 × 150 mm, 1.7 µm) operated in tandem and with a guard column of the same material. Both were maintained at 30 °C. The target analytes were eluted with a flow rate of 0.2 mL min^{-1} and by applying the gradient profile reported by Hopmans et al. (2016). Mass spectrometry conditions followed Bauersachs et al. (2024). The TEX_{86}^{H} index was calculated and converted into sea surface temperature (SST) according to Kim et al. (2010). The branched and isoprenoid tetraether (BIT) index was determined as defined by Hopmans et al. (2004), using the combined peak areas of the 5- and 6-methyl brGDGT isomers. The methyl index was calculated following the methodology of Zhang et al. (2011). Details related to sea surface temperature (SST) reconstructions, as well as all of the datasets used in this study, are described in detail in Bom et al. (2026). Sea surface temperatures (SSTs) were calculated using the TEX_{86}^{H} calibration of Kim et al. (2010), which is expressed as follows:

$$\mathrm{SST}(°\mathrm{C}) = 68.4 \times \log 10(\mathrm{TEX}_{86}) + 38.6, \quad (1)$$

where

$$\mathrm{TEX}_{86} = \frac{\mathrm{GDGT}-2+\mathrm{GDGT}-3+\mathrm{Cren}'}{\mathrm{GDGT}-1+\mathrm{GDGT}-2+\mathrm{GDGT}-3+\mathrm{Cren}'}, \quad (2)$$

and Cren′ represents the regioisomer of crenarchaeol. The TEX_{86}^{H} calibration is recommended for SSTs above 15 °C and has a global calibration error of approximately ±2.5 °C. The Branched and Isoprenoid Tetraether (BIT) index was calculated following Hopmans et al. (2004):

$$\mathrm{BIT} = \frac{\mathrm{Ia}+\mathrm{IIa}+\mathrm{IIIa}}{\mathrm{Ia}+\mathrm{IIa}+\mathrm{IIIa}+\mathrm{Cren}}, \quad (3)$$

where Ia, IIa, and IIIa correspond to the major branched GDGTs, and Cren represents crenarchaeol. All GDGT data used in this study were recently published in Bom et al. (2026); however, the equations are provided here for methodological transparency and reproducibility.

3 Results and discussion

3.1 Planktic foraminiferal analysis

Qualitative and quantitative analyses of upper Maastrichtian–lower Danian planktic foraminifera of the Cerro Azul section revealed well-preserved assemblages (Figs. 2 and 3), allowing for the identification of eight species belonging to six genera and six families (Figs. 2 and 3; see Tables S1 and S2 in the Supplement).

At the Cerro Azul section, we did not observe typical open-marine upper Maastrichtian taxa (e.g. *Abathomphalus* and *Globotruncana*). Instead, only opportunistic long-ranging species, including *Muricohedbergella monmouthensis*, *Guembelitria cretacea*, and *Planoheterohelix globulosa*, occur within the upper Maastrichtian interval. The late Maastrichtian biostratigraphic marker *Plummerita hantkeninoides* is also absent from the Cerro Azul section. This species was recovered from low-latitude upper Maastrichtian sequences in the South Atlantic Ocean, such as the Poty quarry (Koutsoukos, 1996) and Campos Basin (Koutsoukos, 2014). In this context, the absence of typical Maastrichtian planktic foraminiferal marker taxa may be explained by

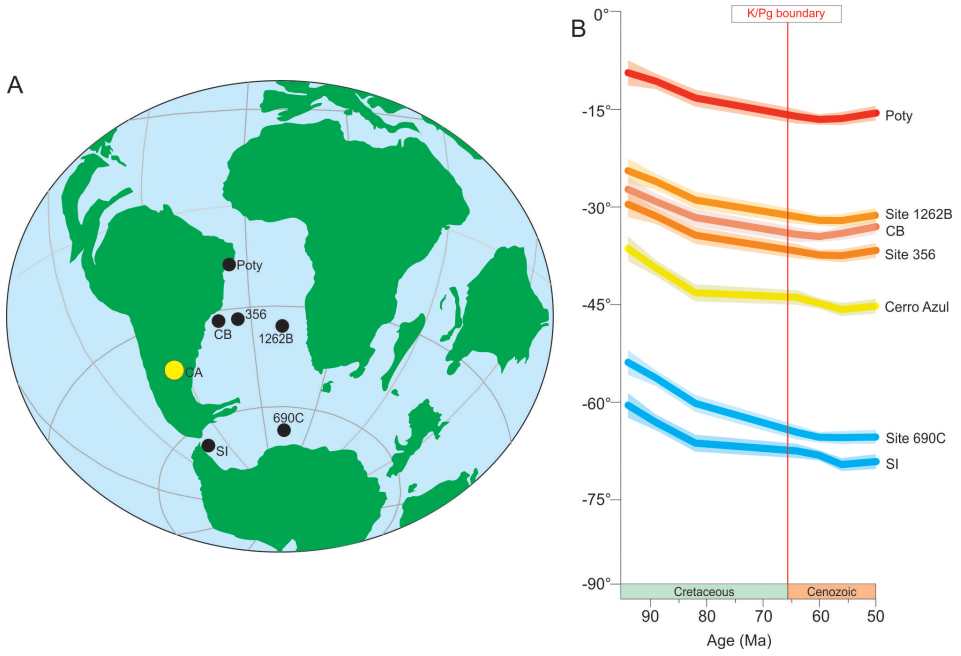

Figure 1. **(A)** Paleogeographic reconstruction of the K–Pg boundary interval (~ 66.0 Ma) (ODSN system: http://www.odsn.de/odsn/services/paleomap/paleomap.html, last access: 30 May 2025). **(B)** Palaeolatitudinal evolution for sites discussed herein during the Cretaceous to Cenozoic interval (~ 95 to 50 Ma), calculated according to Torsvik et al. (2012) and based on the kinematic model of van Hinsbergen et al. (2015) (https://paleolatitude.org, last access: 15 May 2025). CB denotes Campos Basin; SI denotes Seymour Island.

adverse paleoenvironmental conditions in the shallow and semi-restricted Neuquén Basin (e.g. Horton et al., 2016). The stratigraphic completeness of the top of the Maastrichtian sequence cannot be unequivocally confirmed using solely planktic foraminiferal biostratigraphy.

Based on the high-latitude zonal scheme of Huber et al. (2020), two biozones were identified in the lower Danian strata: the AP0 zone and the AP1a subzone (Fig. 4). We adopt herein the high-latitude zonation due to the absence of low-latitude index species (e.g. *Parvularugoglobigerina eugubina*; Berggren et al., 1995) and the high abundance (and regular occurrences) of species endemic to high latitudes (e.g. *Antarcticella pauciloculata*; Huber et al., 2020).

The AP0 zone (partial range of *Turborotalita nikolasi*; Huber et al., 2020) was identified between 16.55 and 17.00 m. The base of this zone was characterised by the last occurrences of typical late Maastrichtian species (i.e. *Planoheterohelix globulosa* and *Muricohedbergella monmouthensis*), which became extinct at the K–Pg boundary. In the first sample of the Danian (16.60 m), the species *Turborotalita nikolasi*, a homonym of the AP0 biozone, was observed. The top of the AP0 zone was placed at 17.00 m based on the first occurrence of the species *Globoconusa daubjergensis*.

The AP1a subzone (*Eoglobigerina eobulloides* partial-range subzone; Huber et al., 2020) has its base defined by the first occurrence of *G. daubjergensis* (17.00 m) and extends upward to the top of the section (17.45 m) due to the absence of typical subzone AP1b forms (i.e. *Subbotina triloculinoides*; Huber and Quillévéré, 2005; Huber et al., 2020).

3.2 Paleoenvironmental changes inferred from planktic foraminiferal assemblages

3.2.1 Upper Maastrichtian

Trochospiral and normal perforate species reported from the upper Maastrichtian of the Cerro Azul section correspond to *Muricohedbergella monmouthensis*. Upper Maastrichtian microperforate species are assigned exclusively to the genuses *Guembelitria* (*Guembelitria cretacea*, *G. dammula*, and *G. blowi*) and *Planoheterohelix* (*P. globulosa*). In the upper Maastrichtian interval of the Cerro Azul section, microperforate *Guembelitria* species present their highest mean total abundances, adding up to 98.1 % (*Guembelitria cretacea* = 66.4 %; *G. blowi* = 20.2 %; *G. dammula* = 11.5 %) at 16.5 m (sample Ca8). The microperforate biserial species *Planoheterohelix globulosa* has a mean total abundance of 0.8 %. Normal perforate taxa show much lower mean total abundance (2.08 %), with the species *Muricohedbergella monmouthensis* at 16.50 m (sample CA8).

3.2.2 Early Danian

In the lowermost Danian (first 15 cm), the highest abundance of microperforate species (97.3 %) is observed, while normal perforate species correspond to only 2.7 % of the assem-

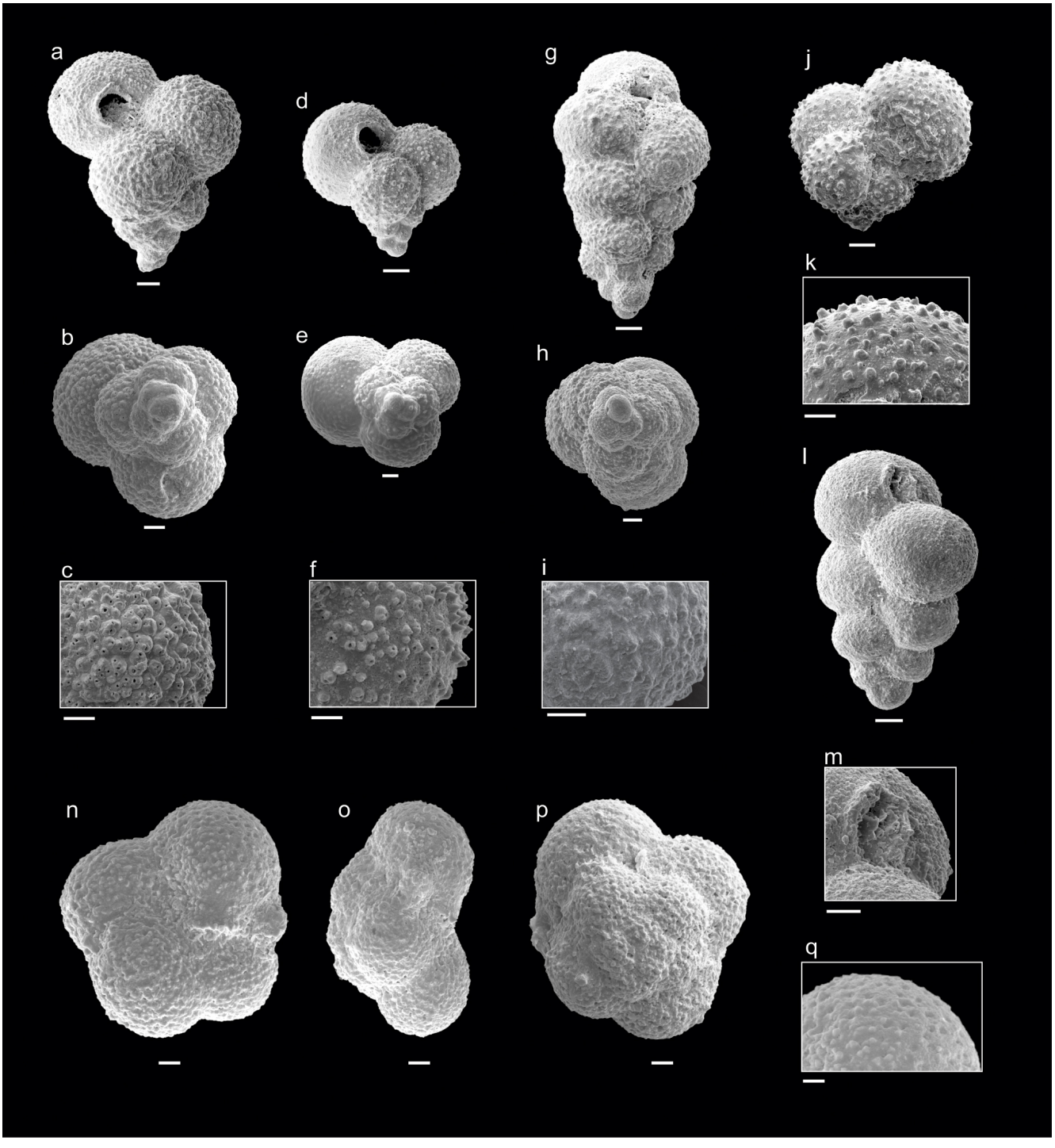

Figure 2. Danian planktic foraminifera from the Cerro Azul section. **(a–c)** *Guembelitria cretacea* (sample Ca9), **(d–f)** *Guembelitria blowi* (sample Ca10), **(g–i)** *Guembelitria dammula* (sample Ca10), **(j–k)** *Globoconusa daubjergensis* (sample Ca13), **(l–m)** *Woodringina claytonensis* (sample Ca16), **(n–q)** *Turborotalita nikolasi* (sample Ca10). Scale bar is 10 µm.

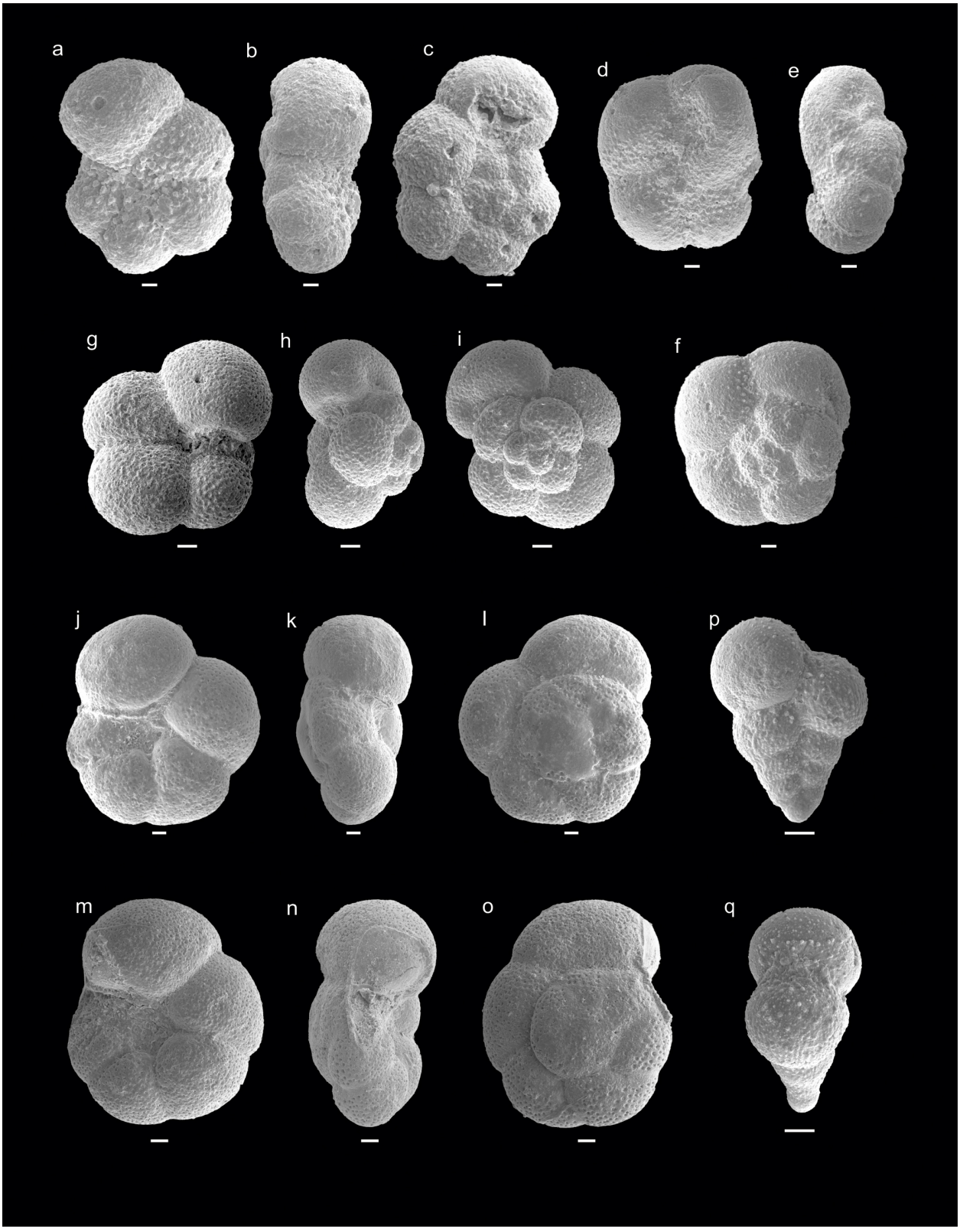

Figure 3. Danian–Maastrichtian planktic foraminifera from Cerro Azul section. **(a–c)** *Antarcticella pauciloculata* (sample Ca9), **(d–f)** *Antarcticella pauciloculata* (sample Ca10), **(g–i)** *Eoglobigerina eobulloides* (sample Ca10), **(j–l)** *Muricohedbergella monmouthensis* (sample Ca8), **(m–o)** *Muricohedbergella monmouthensis* (sample Ca8), **(p–q)** *Planoheterohelix globulosa* (sample Ca10). Scale bar is 10 µm.

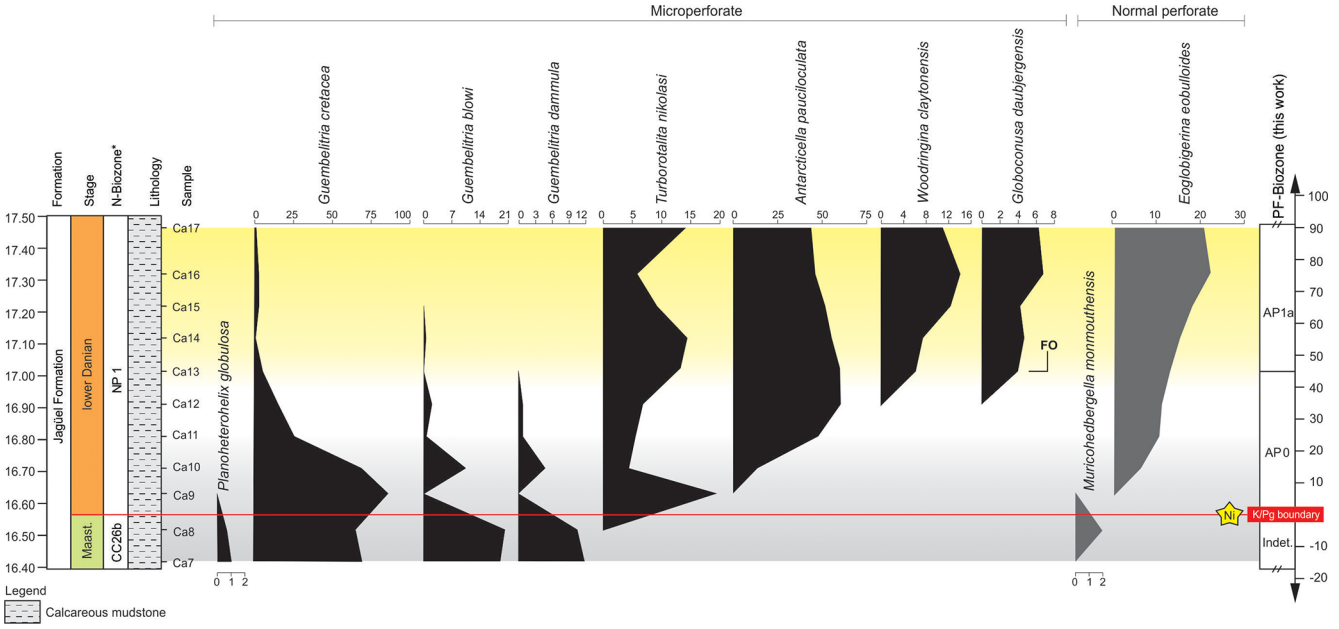

Figure 4. Distribution pattern of planktic foraminifera at the Cerro Azul section across the upper Maastrichtian to lower Danian interval. Intervals: light-grey shading denotes Maastrichtian–Danian boundary instability; yellow shading denotes increased SST and abundance of warm-water dwellings (e.g. *Woodringina claytonensis*). * N-biozones are defined as reported in Guerra et al. (2021), and the position of an Ni spike (star) follows Krahl et al. (2024). Obs.: PF-biozone denotes planktic foraminifera biozone. Relative abundances of planktic foraminifera are expressed as percentages (% of the total assemblage).

blage. In this interval, microperforate species are represented by *Guembelitria cretacea* (74.9 %), *G. blowi* (5.3 %) and *G. dammula* (2.5 %), *Turborotalita nikolasi* (10.7 %), and *Antarcticella pauciloculata* (4.0 %). The mean total abundance of normal perforate specimens for the Danian interval corresponds to 13.8 %, with a progressive increase upward, starting 15 cm above the K–Pg boundary (Fig. 4), and corresponding to the trochospiral and spinose species *Eoglobigerina eobulloides.* The most abundant species in the Danian interval corresponds to *Antarcticella pauciloculata* (42.3 %). The *Antarcticella pauciloculata* species has been reported from Seymour Island, Antarctica (Huber, 1988; Liu et al., 1998), Maud Rise (IODP Site 690C; Liu et al., 1998; Huber et al., 2020); and the Mentelle Basin, southwest of Australia (IODP Site U1514C; Huber et al., 2020). Therefore, its paleogeographic distribution just after the K–Pg boundary in the southern South Atlantic and southern Indian oceans helps to define the extent of the Austral Biogeographic Province (Huber et al., 2020).

The Neuquén Basin record marks the first time that *A. pauciloculata* has been reported outside of the Austral Biogeographic Province, which includes the circum-Antarctic region and New Zealand (Malumían and Náñez, 2011; Ballent et al., 2011), expanding the northernmost boundary of its paleobiogeographic range to mid-latitudes (~ 45° S) in the South Atlantic Ocean. It is particularly abundant in the first metre of the Danian mudstones in the Bajada del Jagüel section (Ballent, 1999). However, at that location, it is unclear how far its range extends into the lowermost Danian because the low-latitude Pα biozone marker species, *Parvularugoglobigerina eugubina*, is absent from the Neuquén Basin. At that section, *A. pauciloculata* was abundantly recovered ~ 5 cm above the K–Pg boundary, within the lower part of biozone AP0 (Fig. 4). At the Cerro Azul section, *A. pauciloculata* occurs just after the K–Pg boundary, together with *Turborotalita nikolasi* (equivalent to an ancestor of the Cenozoic *Praemurica* lineage; Koutsoukos, 2014). It is important to note that higher-resolution sampling (e.g. at the K–Pg boundary and the FO (first occurrence) of *T. nikolasi*) is essential for establishing the accuracy of the FO of *A. pauciloculata*.

The species *Woodringina claytonensis* species occurs 45 cm above the K–Pg boundary and gradually increases in abundance towards the top of the studied interval (Fig. 4). According to D'Hondt and Zachos (1993), *W. claytonensis* exhibits stable oxygen and carbon isotope signatures that indicate a preference for warm, near-surface waters. Additionally, *W. claytonensis* is more abundant in low-latitude open-ocean assemblages (Liu and Olsson, 1992) but is rare at the high latitudes (Liu and Olsson, 1992). Our record of *W. claytonensis* in the Neuquén Basin suggests increased SSTs in zone AP1a (FO *G. daubjergensis*). Increased TEX_{86}^{H}-derived SSTs coeval with high abundances of *W. claytonensis* at the Cerro Azul section support our interpretation (see Sect. 3.3).

Specimens of the genera *Woodringina* and *Parvularugoglobigerina*, which have well-documented evolutionary successions within the early Danian P0 and Pα biozones in

tropical and subtropical, as well as mid-latitude, localities, are absent from southern high-latitude sedimentary successions (Huber et al., 2020). In the Neuquén Basin, the zonal marker species for the Pα zone, *Parvularugoglobigerina eugubina* (sensu Berggren et al., 1995), is absent, as is the *Parvularugoglobigerina* genus in general. To facilitate correlation among southern high-latitude deep-sea sites, Huber and Quillévéré (2005) established an Antarctic Paleocene (AP) zonal scheme, using distinctive species (such as *Turborotalita nikolasi* and *Globoconusa daubjergensis*) that can be reliably correlated among distant circum-Antarctic localities, defining the lower Danian zones AP0 and AP1a.

3.3 Link between sea surface temperature evolution during the early Danian and planktic foraminiferal distributions

Much of our understanding of Danian SSTs comes from calcareous microfossils (planktic foraminifera) recovered from marine sediments (e.g. Quillévéré et al., 2008) and, more recently, from the application of organic temperature proxies, such as the TEX_{86} (Woelders et al., 2017). The TEX_{86} (and its derivatives), based on the distribution of isoprenoid glycerol dialkyl glycerol tetraethers (isoGDGTs) in marine sediments, shows a strong positive correlation with SST (Schouten et al., 2002) and has been frequently applied frequently to study climate and paleoceanographic changes across the K–Pg boundary (e.g. Vellekoop et al., 2014; Woelders et al., 2017).

We reconstructed SSTs using the TEX_{86}^{H} proxy and the calibration function reported by Kim et al. (2010). This approach was employed, as the TEX_{86}^{H} is commonly used to reconstruct SSTs in the Cretaceous (e.g. Woelders et al., 2017), allowing a direct comparison with previously published data (see Table S3). At the Cerro Azul section, SSTs for the first 45 cm of the Danian varied from 28.6 to 29.3° C within the AP0 biozone (Fig. 5). With the start of biozone AP1a ($\sim$ 45 cm above the K–Pg boundary), we observe a $\sim$ 1.5 °C increase in SST. At the transition between biozones AP0 and AP1a, SSTs ranged from 29.8 to 30.7 °C (with an average of around 30.3° C) and decreased slightly towards the top of the studied interval (Fig. 5).

Several proxies have been suggested for testing the reliability of TEX_{86} and its derivatives in paleoenvironmental studies. At the Cerro Azul section, BIT values are generally below 0.2, indicating marine conditions with reduced levels of terrestrial organic matter. Low GDGT-0 / cren ratios (< 0.2) suggest only a negligible contribution of isoGDGTs from methanogens (Zell et al., 2014), while low GDGT-2 / GDGT-3 ratios, varying from 1.03 to 2.81 (with an average of 1.52 ± 0.62), are indicative of a predominant surface water production of GDGTs (Hernández-Sánchez et al., 2014). In addition, methane index values between 0.13 to 0.33 (average 0.24 ± 0.06) at the Cerro Azul section suggest no significant impact of GDGTs derived from methanotrophic archaea on the calculation of the TEX_{86}^{H} (Zhang et al., 2011). Together, these observations suggest that the TEX_{86}^{H} is not significantly affected by environmental and biological factors other than temperature and yields robust SST reconstructions for the Cerro Azul section.

Increased SSTs during the earliest Danian have been reported within different low-latitude biozones: biozone P1a on the Blake Nose Plateau, with an SST rise of $\sim$ 4.0 °C during the Dan-C2 event depicted by planktic foraminiferal oxygen isotope values (Ocean Drilling Program Site 1049; Quillévéré et al., 2008) and in the Tethys (Contessa Highway; Coccioni et al., 2010); in biozone P1b on the Rio Grande Rise (Deep Sea Drilling Program Site 516; Krahl et al., 2020) and the Walvis Ridge (ODP Site 1262; Krahl et al., 2023); and in parts of biozones P1a and P1b at the Caravaca section (Gilabert et al., 2021a). Increased SSTs recorded at the Cerro Azul section occur within biozone AP1a. According to Huber and Quillévéré (2005), the FO of *G. daubjergensis* is placed in the upper part of Chron C29r at ODP Holes 690C (Falkland) and 738C (Kergelen Plateau). In this context, the increase in SST observed at the Cerro Azul section may likely represent the Dan-C2 event, as described by Quillévéré et al. (2008).

Increased SSTs at the Cerro Azul section correlate with a moderate increase in the abundance of *W. claytonensis* 45 cm above the K–Pg boundary (Fig. 4). This increase in the abundance of *W. claytonensis* appears to agree with the slight decreases in abundances of *Antarcticella paucilocu-lata*. This foraminiferal species was more abundant in low-latitude open-ocean assemblages than in high-latitude open-marine environments (D'Hondt and Keller, 1991; Liu and Olsson, 1992). Specifically, no *Woodringina* species has been reported in high-latitude sections yet (Huber, 1996, 1988; Huber et al., 2020). For mid-latitudes in the South Atlantic Ocean, the presence of the *Woodringina* genus (*W. claytonensis* and *W. hornerstownensis*) was observed for the early Danian of the São Paulo Plateau (DSDP Site 356; Krahl et al., 2017), the Campos Basin (Brazil; Koutsoukos, 2014), and the Walvis Ridge (ODP Site 1262; Krahl et al., 2023). The paleogeographical position of the Neuquén Basin ($\sim$ 45° S: van Hinsbergen et al., 2015) was intermediate between these occurrences and high-latitude faunas (Fig. 1). In this context, we suggest that the presence of *W. claytonensis* at the Cerro Azul section may have been related to latitudinal migration due to increased SSTs.

4 Conclusions

The shallow marine sequence at the Cerro Azul section (Neuquén Basin, Argentina) reveals a sedimentary succession with well-preserved planktic foraminifera spanning the upper Maastrichtian to the lower Danian interval. We recognise two early Danian planktonic foraminiferal biozones at the Cerro Azul: AP0 (partial range of *Turborotalita niko-*

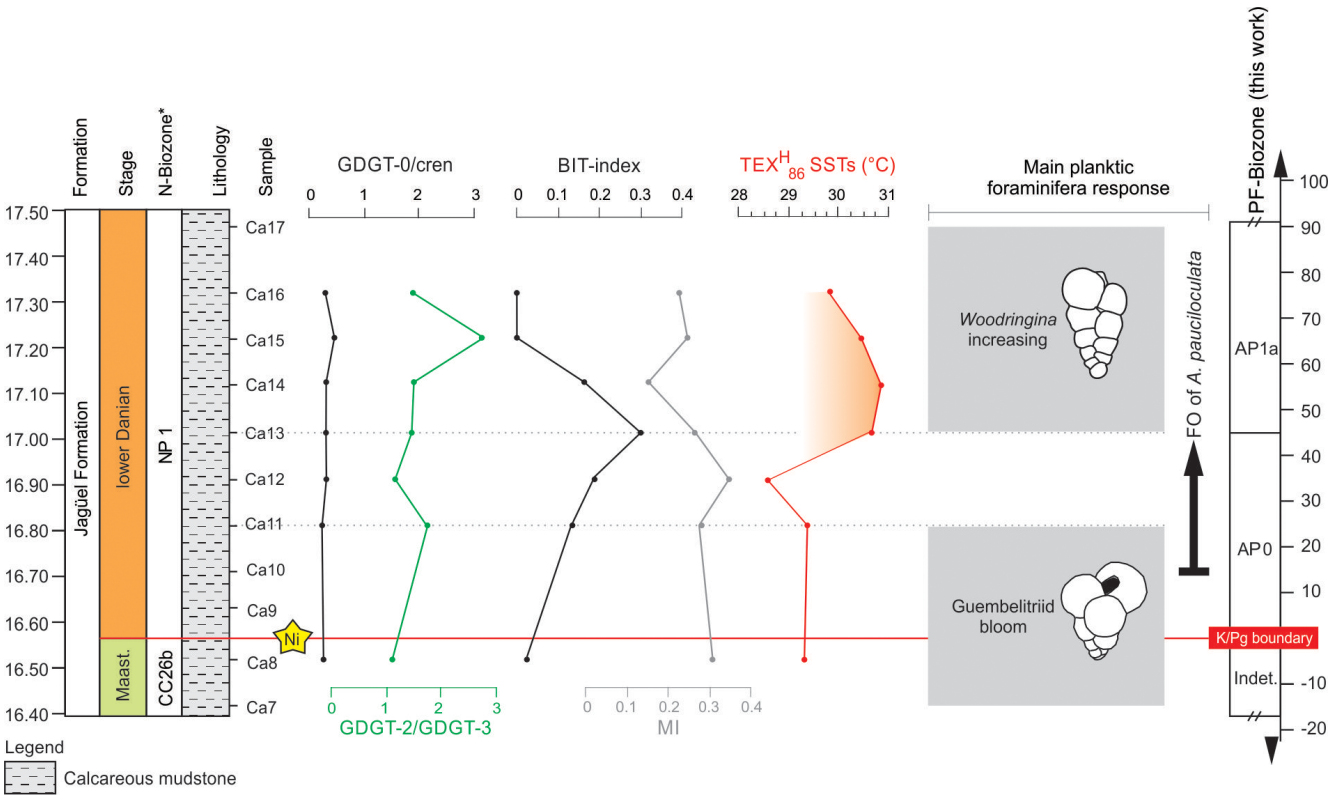

Figure 5. Records of the GDGT-0 / cren ratio, GDGT-2 / GDGT-3 ratio, BIT index, methane index (MI), and TEX$^{H}_{86}$ SSTs at the Cerro Azul section. The response of planktic foraminiferal assemblages is shown to the right (Guembelitriid bloom refers to *Guembelitria cretacea*, *G. dammula*, and *G. blowi*). Nannofossil (N-) biozones follow Guerra et al. (2021), and planktic foraminiferal (PF-) biozones were defined in this work. * FO denotes first occurrence.

lasi) and AP1a (*Eoglobigerina eobulloides* partial-range subzone), which are characteristic of high-latitude assemblages. Maastrichtian biostratigraphic markers are absent from the Cerro Azul section, likely due to adverse paleoenvironmental conditions in the shallow and semi-restricted Neuquén Basin.

Abundant opportunistic taxa that thrived under paleoenvironmental instability were observed across the K–Pg boundary (e.g. *Guembelitria* genus). Approximately 45 cm above the K–Pg boundary, the Cerro Azul section records a rapid SST 265 increase of 1.5° C, associated with moderately increased abundances of *W. claytonensis*, which may represent immigration from lower and warmer latitudes. Planktic foraminiferal assemblages in the beginning of the Danian at the Cerro Azul section presented a mid-to-high-latitude affinity based on the occurrence of *Antarcticella pauciloculata*, whose paleobiogeographic range in the South Atlantic Ocean is extended herein to mid-latitudes.

Data availability. All datasets discussed in the present work are available in Tables S1, S2, and S3 in the Supplement.

- *Table S1.* Foraminifera taxa recorded in Cerro Azul section (count specimens).
- *Table S2.* Foraminifera taxa recorded in Cerro Azul section (specimens in percentages; %).
- *Table S3.* Organic geochemistry data for the Cerro Azul: GDGT-0/cren, GDG-2/GDGT-3, BIT index, MI, and TEX$^{H}_{86}$ SSTs (°C). The database used for the temperature calculations, as well as detailed procedures and methodological considerations, are described in Bom et al. (2026).

Sample availability. The studied samples are stored at the Technological Institute for Paleoceanography and Climate Change (itt OCEANEON), UNISINOS University, Brazil. Specimens figured herein are housed in the repository of Paleontological Collection of the University of Buenos Aires, Argentina (curatorial numbers (LM-FCEN) are given after each specimen in Figs. 2 and 3).

Supplement. The supplement related to this article is available online at https://doi.org/10.5194/jm-45-297-2026-supplement.

Author contributions. Samples were collected by AC, TM, and DC. The initial draft was written, with subsequent revisions and interpretations, by GK, KGDK, MHHB, RMG, TB, LS, and GF.

All of the authors of the paper collaborated in the text revisions and discussions.

Competing interests. The contact author has declared that none of the authors has any competing interests.

Disclaimer. Publisher's note: Copernicus Publications remains neutral with regard to jurisdictional claims made in the text, published maps, institutional affiliations, or any other geographical representation in this paper. The authors bear the ultimate responsibility for providing appropriate place names. Views expressed in the text are those of the authors and do not necessarily reflect the views of the publisher.

Acknowledgements. The authors are grateful to Brian Huber, Lizette Leon-Rodriguez, and one anonymous referee for their valuable comments, which greatly improved the first version of the paper.

Financial support. This research has been supported by the National Council for Scientific and Technological Development (CNPq) (grant no. 307309/2023-1). Additional contribution R-518 from the Institute of Andean Studies "Don Pablo Groeber".

Review statement. This paper was edited by Sev Kender and reviewed by Brian Huber, Lizette Leon-Rodriguez, and one anonymous referee.

References

Arenillas, I., Arz, J. A., and Gilabert, V.: Blooms of aberrant planktic foraminifera across the K/Pg boundary in the Western Tethys: causes and evolutionary implications, Paleobiology, 3, 1–17, https://doi.org/10.1017/pab.2018.16, 2018.

Arenillas, I., Arz, J. A., Molina, E., and Dupuis, C.: An independent test of planktic foraminiferal turnover across the Cretaceous/Paleogene (K/P) boundary at El Kef, Tunisia: Catastrophic mass extinction and possible survivorship, Micropaleontology, 46, 31–49, https://www.jstor.org/stable/1486024 (last access: 10 October 2024), 2000.

Aze, T., Ezard, T. H. G., Purvis, A., Coxall, H. K., Stewart, R. M., Wade, B. S., and Pearson, P. N.: A phylogeny of Cenozoic macroperforate planktonic foraminifera from fossil data, Biol. Rev., 86, 900–927, https://doi.org/10.1111/j.1469185X.2011.00178.x, 2011.

Ballent, S. C.: Foraminíferos del Jurásico medio (Límite Aaleniense-Bajociense) del centro-oeste de Argentina, Sistemática. Revista Española de Micropaleontolgía, 31, 123–147, 1999.

Ballent, S., Concheyro, A., Náñez, C., Pujana, I., Lescano, M., Carignano, A. P., Caramés, A., Angelozzi, G., and Ronchi, D.: Microfósiles Mesozoicos y Cenozoicos, in: Relatorio del XVIII Congreso Geológico Argentino, Neuquén, Argentina, 489–528, ISBN 978-987-22403-3-2, 2011.

Bauersachs, T., Schubert, C. J., Mayr, C., Gilli, A., and Schwark, L.: Branched GDGT-based temperature calibrations from Central European lakes, Sci. Total Environ., 906, 167724, https://doi.org/10.1016/j.scitotenv.2023.167724, 2024.

Berggren, W. A.: Rates of evolution in some Cenozoic planktonic foraminifera, Micropaleontology, 15, 351–365, https://doi.org/10.2307/1484931, 1969.

Berggren, W. A., Kent, D. V., Swisher III, C. C., and Aubry, M. P.: A revised Cenozoic geochronology and chronostratigraphy, in: Geochronology, Time Scales and Global Stratigraphic Correlations, edited by: Berggren, W. A., Kent, D. V., Aubry, M. P., and Hardenbol, J., Special publication Society for Sedimentary Geology), 129–212, https://doi.org/10.2110/pec.95.04.0129, 1995.

Bertels, A.: Micropaleontología del Paleoceno de General Roca (provincia de Río Negro, República Argentina), Revista Museo La Plata, 4, 125–184, 1964.

Bertels, A.: Micropaleontología y estratigrafía del límite Cretácico-Terciario en Huantraico, provincia del Neuquén, Ameghiniana, 4, 253–278, 1969a.

Bertels, A.: Estratigrafía del límite Cretácico-Terciario en la Patagonia septentrional, Revista de la Asociación Geológica Argentina, 24, 41–54, 1969b.

Bertels, A.: Los foraminíferos planctónicos de la cuenca cretácica-terciaria en Patagonia septentrional (Argentina) con consideraciones sobre la estratigrafía de General Roca (provincia de Río Negro), Ameghiniana, 7, 1–56, 1970.

Bertels, A.: Buliminacea y Cassidulinacea (Foraminiferida) guías del Cretácico superior (Maastrichtia no medio) y Terciario inferior (Daniano inferior) de la República Argentina, Revista Española de Micropaleontología, 4, 327–353, 1972.

Bertels, A.: Upper Cretaceous (lower Maastrichtian) ostracodes from Argentina, Micropaleontology, 4, 385–397, https://doi.org/10.2307/1485126, 1974.

Bertels, A.: Bioestratigrafía del Paleógeno en la República Argentina, Revista Española de Micropaleontología, 7, 429–450, 1975a.

Bertels, A.: Upper Cretaceous (middle Maastrichtian) ostracodes of Argentina, Micropaleontology, 21, 97–130, https://doi.org/10.2307/1485157, 1975b.

Bom, M. H., Kochhann, K. G. D., Guerra, R. M., Ceolin, D., Krahl, G., Duarte, L. R., Pacheco, M., Bauersachs, T., Rodrigues, L. F., Callefo, F., Trentin, F. A., Galante, D., Musso, T., Schwark, L., Concheyro, A., and Fauth, G.: Early Danian paleotemperature records from Neuquén Basin-Argentina: Applications of the ostracod Sr/Ca paleothermometer, Evolving Earth, 4, 100113, https://doi.org/10.1016/j.eve.2026.100113, 2026.

Ceolin, D., Whatley, R. D., Fauth, G., and Concheyro, A.: New genera and species of Ostradoda from the Maastrichtian and Danian of the Neuquén Basin, Argentina, Papers in Paleontology, 4, 425–495, https://doi.org/10.1002/spp2.1023, 2015.

Ceolin, D., Whatley, R., Fauth, G., and Concheyro, A.: The Nodoconchiinae, a new subfamily of Cytheridae (Crustacea, Ostracoda), J. Micropalaeontol., 35, 90–101, https://doi.org/10.1144/jmpaleo2015-003, 2016.

Coccioni, R., Frontalini, F., Bancalà, G., Fornaciari, E., Jovane, L., and Sprovieri, M.: The Dan-C2 hyperthermal event at Gubbio (Italy): Global implications, environmental ef-

fects, and cause(s), Earth Planet. Sc. Lett., 297, 298–305, https://doi.org/10.1016/j.epsl.2010.06.031, 2010.

D'Hondt, S. and Keller, G.: Some patterns of planktic foraminiferal assemblage turnover at the CretaceousTertiary boundary, Mar. Micropaleontol., 17, 77–118, https://doi.org/10.1016/0377-8398(91)90024-Z, 1991.

D'Hondt, S. and Zachos, J. C.: On Stable Isotopic Variation and Earliest Paleocene Planktonic Foraminifera, Palaeoceanography, 8, 527–547, https://doi.org/10.1029/93PA00952, 1993.

Gilabert, V., Arenillas, I., Arz, J. A., Batenburg, S. J., and Robinson, S. A.: Multiproxy analysis of paleoenvironmental, paleoclimatic and paleoceanographic changes during the early Danian in the Caravaca section (Spain), Palaeogeogr. Palaeocl., 110513, https://doi.org/10.1016/j.palaeo.2021.110513, 2021a.

Gilabert, V., Batenburg, S. J., Arenillas, I., and Arz, J. A.: Contribution of orbital forcing and Deccan volcanism to global climatic and biotic changes across the Cretaceous-Paleogene boundary at Zumaia, Spain, Geology, 50, 21–25, https://doi.org/10.1130/G49214.1, 2021b.

Guerra, R. M., Concheyro, A., Kochhann, K. G. D., Bom, M. H. H., Ceolin, D., Musso, T., Savian, J. F., and Fauth, G.: Calcareous microfossils and paleoenvironmental changes across the Cretaceous-Paleogene (K-Pg) boundary at the Cerro Azul Section, Neuquén Basin, Argentina, Palaeogeogr. Palaeocl., 567, 1–13, https://doi.org/10.1016/j.palaeo.2021.110217, 2021.

Hernández-Sánchez, M. T., Woodward, E. M. S., Taylor, K. W. R., Henderson, G. M., and Pancost, R. D.: Variations in GDGT distributions through the water column in the South East Atlantic Ocean, Geochim. Cosmochim. Ac., 132, 337–348, https://doi.org/10.1016/j.gca.2014.02.009, 2014.

Hopmans, E. C., Weijers, J. W. H., Schefuß, E., Herfort, L., and Damsté, J. S. S., and Schouten, S.: A novel proxy for terrestrial organic matter in sediments based on branched and isoprenoid tetraether lipids, Earth Planet. Sc. Lett., 224, 107–116, https://doi.org/10.1016/j.epsl.2004.05.012, 2004.

Hopmans, E. C., Schouten, S., and Damsté, J. S. S.: The effect of improved chromatography on GDGT-based palaeoproxies, Org. Geochem., 93, 1–6, https://doi.org/10.1016/j.orggeochem.2015.12.006, 2016.

Horton, B. K., Fuentes, F., Boll, A., Starck, D., Ramirez, S. G., and Stockli, D.: Andean stratigraphic record of the transition from backarc extension to orogenic shortening: A case study from the northern Neuquen Basin, Argentina, J. S. Am. Earth Sci., 71, 17–40, https://doi.org/10.1016/j.jsames.2016.06.003, 2016.

Huber, B. T.: Upper Campanian-Paleocene foraminifera from the James Ross Island region (Antarctic Peninsula), in Geology and Paleontology of Seymour Island, Antarctica Peninsula, edited by: Feldmann, R. M. and Woodburne, M. O., Geol. Soc. Am. Mem., 163–251, https://doi.org/10.1130/MEM169-p163, 1988.

Huber, B. T.: Evidence for planktonic foraminifer reworking vs. survivorship across the Cretaceous/Tertiary boundary at high latitudes, in: The Cretaceous-Tertiary Event and Other Catastrophes in Earth History, edited by: Ryder, G., Fastovsky, D., and Gartner, S., Boulder, CO, Geol. Soc. Am. Spec. Paper, 307, 319–334, https://doi.org/10.1130/0-8137-2307- 8.319, 1996.

Huber, B. T. and Quillévéré, F.: Revised Paleogene planktonic foraminiferal biozonation for the Austral Realm, J. Foramin. Res., 35, 299–314, https://doi.org/10.2113/35.4.299, 2005.

Huber, B., Petrizzo, M. R., and MacLeod, K.: Planktonic Foraminiferal Endemism at Southern High Latitudes Following the Terminal Cretaceous Extinction, J. Foramin. Res., 4, 382–402, doi.org/10.2113/gsjfr.50.4.382, 2020.

Keller, G., Li, L., and MacLeod, N.: The Cretaceous/Tertiary boundary stratotype section at E1 Kef, Tunisia: how catastrophic was the mass extinction?, Palaeogeogr. Palaeocl., 119, 221–254, https://doi.org/10.1016/0031-0182(95)00009-7, 1996.

Keller, G., Adatte, T., Tantawy, A. A., Berner, Z., Stinnesback, W., Stueben, D., and Leanza, H. A.: High stress late Maastrichtian e early Danian palaeoenvironment in the Neuquen Basin, Argentina, Cretaceous Res., 6, 939–690, https://doi.org/10.1016/j.cretres.2007.01.006, 2007.

Kim, J., van der Meer, J., Schouter, S., Helmke, P., Willmott, V., Sangiorgi, F., Koç, N., Hopmans, E. C., and Damsté, J. S. S.: New indices and calibrations derived from the distribution of crenarchaeal isoprenoid tetraether lipids: Implications for past sea surface temperature reconstructions, Geochim. Cosmochim. Ac., 16, 4639–4635, https://doi.org/10.1016/j.gca.2010.05.027, 2010.

Koutsoukos, E. A. M.: The Cretaceous-Tertiary boundary at Poty, NE Brazil-event stratigraphy and palaeoenvironments, B. Cent. Rech. Expl., 16, 413–431, 1996.

Koutsoukos, E. A. M.: Phenotypic plasticity, speciation, and phylogeny in early Danian planktic foraminífera, J. Foramin. Res., 2, 109–142, https://doi.org/10.2113/gsjfr.44.2.109, 2014.

Krahl, G., Koutsoukos, E. A. M., and Fauth, G.: Paleocene planktonic foraminifera from DSDP Site 356, South Atlantic: Paleoceanographic inferences, Mar. Micropaleontol., 135,1–14, https://doi.org/10.1016/j.marmicro.2017.07.001, 2017.

Krahl, G., Bom, M. H. H., Kochhann, K. G. D., Souza, L. V., Savian, J. F., and Fauth, G.: Environmental changes occurred during the early Danian at the Rio Grande Rise, South Atlantic Ocean, Global Planet. Change, 191, 103197, https://doi.org/10.1016/j.gloplacha.2020.1 03197, 2020.

Krahl, G., Arenillas, I., Gilabert, V., Kochhann, K. G. D., Bom, M. H. H., Fauth, G., and Arz, J. A.: Impact of early Danian environmental perturbations on mid-latitude planktic foraminifera assemblages from ODP Site 1262 (South Atlantic Ocean), Newsl. Stratigr., 56, 377–403, https://doi.org/10.1127/nos/2023/074, 2023.

Krahl, G., Concheyro, A., Bom, M. H. H., Musso, T., Guerra, R. M., Ceolin, D., Kochhann, K. G. D., and Fauth, G.: Planktic foraminiferal biostratigraphy across the upper Maastrichtian-early Danian in the Neuquén basin (Cerro Azul section), in: Actas XXII Congreso Geológico Argentino, San Luis, Argentina, 1029–1030, ISBN 978-987-48319-2-7, 2024.

Kroon, D. and Nederbragt, A. J.: Ecology and paleoecology of triserial planktic foraminifera, Mar. Micropaleontol., 16, 25–38, doi.org/10.1016/0377-8398(90)90027-j, 1990.

Liu, C. and Olsson, R. K.: Evolutionary adaptive radiation of microperforate planktonic foraminifera following the K/T mass extinction event, J. Foramin. Res., 22, 328–346, https://doi.org/10.2113/gsjfr.22.4.328, 1992.

Liu, C., Olsson, R. K., and Huber, B. T.: A benthic paleohabitat for Praeparatotalia gen. nov. and Antarcticella Loeblich and Tappan, J. Foramin. Res., 28, 75–90, 1998.

Lowery, C. M., Bown, P. R., Fraass, A. J., and Hull, P. M., 2020, Ecological response of plankton to environmental change:

Thresholds for extinction: Annu. Rev. Earth Pl. Sci., 48, 403–429, 10.1146/annurev-earth-081619-052818, 2020.

Lowery, C. M., Jones, H. L., Bralower, T., Cruz, L. P., Gebhardt, C., Whalen, M. T., Chenot, E., Smit, J., Phillips, M. P., Choumiline, K., Arenillas, I., Arz, J. A., Garcia, F., Ferrand, M., Lofi J., and Gulick, S. P. S.: Early Paleocene Paleoceanography and Export Productivity in the Chicxulub Crater, Paleoceanogr. Paleocl., 36, e2020PA004241, https://doi.org/10.1029/2020PA004241, 2021.

Malumían, N. and Náñez, C.: The Late Cretaceous-Cenozoic transgressions in Patagonia and the Fuegian Andes: foraminifera, palaeoecology, and palaeogeography, Biol. J. Linn. Soc., 103, 269–288, https://doi.org/10.1111/j.1095- 8312.2011.01649.x, 2011.

Molina, E.: Evidence and causes of the main extinction events in the Paleogene based on extinction and survival patterns of foraminifera, Earth-Sci. Rev., 140, 166–181, https://doi.org/10.1016/j.earscirev.2014.11.008, 2015.

Musso, T., Cocheyro, A., and Pettanari, G.: Clay mineralogy and calcareous nannofossils from Jagüel and Roca formations in the eastern sector of Pellegrini Lake, Neuquen Basin, República Argentina, Andean Geol., 39, 511–540, https://doi.org/10.5027/andgeoV39n3-a08, 2012.

Nañez, C. and Concheyro, A.: Limite Cretacico-Paleogeno. Geologia y Recursos Minerales del departamento Añelo, Proíncia del Neuquén, República Argentina, Anales de la Dirección Nacional del Servicio Geológico, 129–150, 1996.

Olsson, R. K., Hemleben, C., Berggren, W. A., and Huber, B. T.: Atlas of Paleocene Planktonic Foraminifera, in: Smithsonian Contribution to Paleobiology, edited by: Olsson, R. K., Hemleben, C., Berggren, W. A., and Huber, B. T., 85, 1–252, https://doi.org/10.5479/si.00810266.85.1, 1999.

Pardo, A. and Keller, G.: Biotic effects of environmental catastrophes at the end of the Cretaceous and early Tertiary: Guembelitria and Heterohelix blooms, Cretaceous Res., 29, 1058–1073, doi.org/10.1016/j.cretres.2008.05.031, 2008.

Pincheira, E. P. and di Pasquo, M.: Palynology of the Jagüel Formation (Maastrichtian–Danian) in northwestern Río Negro, Neuquén Basin, Argentina: paleobiogeographic inferences, Cretaceous Res., 127, 104932, https://doi.org/10.1016/j.cretres.2021.104932, 2021.

Punekar, J., Mateo, P., and Keller, G.: Effects of Deccan volcanism on paleoenvironment and planktic foraminifera: A global survey, in: Volcanism, Impacts, and Mass Extinctions: Causes and Effects, edited by: Keller, G. and Kerr, A. C., Geol. Soc. Am. Spec. Paper, 505, 91–116, https://doi.org/10.1130/2014.2505(04), 2014.

Quillévéré, F., Norris, R. D., Kroon, D., and Wilson, P. A.: Transient ocean warming and shifts in carbon reservoirs during the early Danian, Earth Planet. Sc. Lett., 265, 600–615, https://doi.org/10.1016/j.epsl.2007.10.040, 2008.

Schouten, S., Hopmans, E. C., Schefuß, E., and Sinninghe Damsté, J. S.: Distributional variations in marine crenarchaeotal membrane lipids: A new tool for reconstructing ancient sea water temperatures?, Earth Planet. Sc. Lett., 204, 265–74, https://doi.org/10.1016/S0012-821X(02)00979-2, 2002.

Stott, L. D. and Kennett, J. P.: Antarctic Paleogene planktonic foraminifer biostratigraphy: ODP Leg 113 sites 689 and 690, in: Proceedings of the Ocean Drilling Program, Scientific Results: Ocean Drilling Program, edited by: Barker, P. F., College Station, Texas, 549–569, https://doi.org/10.2973/odp.proc.sr.113.121.1990, 1990.

Torsvik, T. H., Van der Voo, R., Preeden, U., MacNiocaill, C., Steinberger, B., Doubrovine, P., van Hinsbergen, D. J. J., Domeier, M., Gaina, C., Tohver, E., Meert, J. G., McCausland, P. J. A., and Cocks, L. R. M.: Phanerozoic polar wander, palaeogeography and dynamics, Earth-Sci. Rev., 114, 325–368, https://doi.org/10.1016/j.earscirev.2012.06.007, 2012.

Wade, B. S., Pearson, P. N., Berggren, W. A., and Pälike, H.: Review and revision of Cenozoic tropical planktonic foraminiferal biostratigraphy and calibration to the geomagnetic polarity and astronomical time scale, Earth Sci. Rev., 104, 111–142, https://doi.org/10.1016/j.earscirev.2010.09.003, 2011.

Woelders, L., Vellekoop, J., Kroon, D., Smit, J. Casadío, S., Prámparo, M. B., Dinerès-Turell, J., Peterse, F., Sluijs, A., Lenaerts, J. T. M., and Speijer, R. P.: Latest Cretaceous climatic and environmental change in the South Atlantic region, Paleoceanography, 32, 466–483, https://doi.org/10.1002/2016PA003007, 2017.

Vandenberghe, N., Hilgen, F. J., and Speijer, R. P.: The Paleogene Period, in: The Geologic Time Scale 2012, edited by: Gradstein, F. M., Ogg, J. G., Schmits, P., and Ogg, G., Elsevier, 855–921, https://doi.org/10.1016/B978-0-444-59425-9.00028-7, 2012.

van Hinsbergen, D. J. J., de Groot, L. V., van Schaik, S. J., Spakman, W., Bijl, P. K., Sluijs, A., Langereis, C. G., and Brinkhuis, H.: A Paleolatitude Calculator for Paleoclimate Studies, PLoS ONE, 10, e0126946, https://doi.org/10.1371/journal.pone.0126946, 2015.

Vellekoop, J., Sluijs, A., Smit, J., and Brinkhuis, H.: Rapid short-term cooling following the Chicxulub impact at the Cretaceous–Paleogene boundary, P. Natl. Acad. Sci. USA, 111, 7537–7541, https://doi.org/10.1073/pnas.1319253111, 2014.

Zhang, Y. G., Zhang, C. L., Liu, X., Li, L., Hinrichs, K., and Noakes, J. E.: Methane Index: A tetraether archaeal lipid biomarker indicator for detecting the instability of marine gas hydrates, Earth Planet. Sc. Lett., 307, 525–534, https://doi.org/10.1016/j.epsl.2011.05.031, 2011.

Zell, C., Kim, J. H., Hollander, D., Lorenzoni, L., Baker, P., Silva, C. G., Nittrouer, C., and Damsté, J. S. S.: Sources and distributions of branched and isoprenoid tetraether lipids on the Amazon shelf and fan: Implications for the use of GDGT-based proxies in marine sediments, Geochim. Cosmochim. Ac., 139, 293–312, https://doi.org/10.1016/j.gca.2014.04.038, 2014.